G-quadruplex formation at the 3′ end of telomere DNA inhibits its extension by telomerase, polymerase and unwinding by helicase

Quan Wang[1], Jia-quan Liu[2], Zhao Chen[2], Ke-wei Zheng[2], Chang-yue Chen[2], Yu-hua Hao[1] and Zheng Tan[1,*]

[1]State Key Laboratory of Biomembrane and Membrane Biotechnology, Institute of Zoology, Chinese Academy of Sciences, Beijing 100101 and [2]Laboratory of Biochemistry and Biophysics, College of Life Sciences, Wuhan University, Wuhan 430072, PR China

ABSTRACT

Telomere G-quadruplex is emerging as a promising anti-cancer target due to its inhibition to telomerase, an enzyme expressed in more than 85% tumors. Telomerase-mediated telomere extension and some other reactions require a free 3′ telomere end in single-stranded form. G-quadruplex formation near the 3′ end of telomere DNA can leave a 3′ single-stranded tail of various sizes. How these terminal structures affect reactions at telomere end is not clear. In this work, we studied the 3′ tail size-dependence of telomere extension by either telomerase or the alternative lengthening of telomere (ALT) mechanism as well as telomere G-quadruplex unwinding. We show that these reactions require a minimal tail of 8, 12 and 6 nt, respectively. Since we have shown that G-quadruplex tends to form at the farthest 3′ distal end of telomere DNA leaving a tail of no more than 5 nt, these results imply that G-quadruplex formation may play a role in regulating reactions at the telomere ends and, as a result, serve as effective drug target for intervening telomere function.

INTRODUCTION

Human chromosomes are protected at both ends with repetitive T_2AG_3 tracks that terminate with a ∼200-nt single-stranded G-rich overhang beyond the double-stranded region (1–4) Telomere DNA in human cells shortens during each round of chromosome replication due to the end-replication problem (5,6). In >85%

cancer cells, the telomere shortening is compensated by telomerase that add nucleotides to telomere ends to maintain telomere length and the proliferative potential of the cells (7). Using a minimum of four T_2AG_3 repeats telomere DNA can fold into a four-stranded structure known as G-quadruplex that can inhibit telomerase (8). For this reason, stabilization of G-quadruplex by small molecule drugs is regarded as a promising anti-cancer therapy (9). Due to the repetitive nature of telomere DNA, a telomere overhang may carry a single-stranded G-rich 3′ tail of zero to three intact T_2AG_3 repeats at the 3′ side of the farthest distal G-quadruplex (10). Although G-quadruplex *per se* is inhibitory to telomerase activity, how G-quadruplexes with 3′ tails of different sizes are processed by telomerase and other enzymes has not been studied. Apparently whether a 3′ tail is extendable by telomerase may well depend on the tail size. A G-quadruplex at the very 3′ end may fully inhibit extension while a G-quadruplex away from the 3′ end with sufficient 3′ tail length may not be inhibitory (Figure 1). Besides the telomerase-mediated telomere extension, the G-quadruplex position at the 3′ end may also affect other reactions that require a free 3′ telomere end and, as a consequence, influence the relevant biological functions.

In this work, we studied how the size of a 3′ telomere tail flanking a telomere G-quadruplex affects telomere extension by telomerase and the alternative lengthening of telomere (ALT) mechanism, as well as the unwinding of quadruplex by helicase. Our results show that these reactions require a minimal 3′ tail of 8, 12 and 6 nt, respectively. We have shown previously that G-quadruplex preferentially forms at the very 3′ end of telomere DNA with higher occurring frequency when it can form at multiple positions (10). Since a G-quadruplex at the
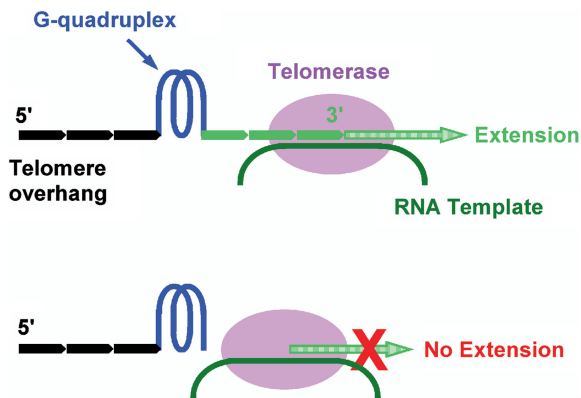
Figure 1. Extension of telomere by telomerase depends on the size of single-stranded tail at the 3′ side of the farthest distal G-quadruplex on telomere overhang. A telomere tail of less than four T_2AG_3 repeats (0–23 nt) will stay in single-stranded form. Those with tails long enough but unable to form G-quadruplex can be extended (top) while others without or with too short tails may not be extended (bottom).

farthest possible 3′ end of telomere DNA will have a 3′ tail of no more than 5 nt (TTAGG), our results argue that G-quadruplex formation on telomere overhang can inhibit such telomere end processing reactions that require a free 3′ tail. Therefore, we propose that G-quadruplex can play a role in regulating telomere end processing and, as a result, serve as effective drug target for intervening telomere function.

MATERIALS AND METHODS

Telomere extension by telomerase

Telomerase activity was assayed using reconstituted human telomerase (11,12) and the TRAP-G4 method (13) with a TSNT internal standard (IS) (14,15). Briefly, hTR RNA was transcribed using the T7 transcription kit (Fermentas, Lithuania) and double-stranded (dsDNA) template amplified from nucleotides +1–+388 in the plasmid pUC119-hTR(+1–451) with sense primer 5′-CC CCAGGCTTTACACTTTATGC and antisense primer 5′-ACTCGCTCCGTTCCTCTTCC. hTERT was expressed using the TnT quick coupled transcription/translation kit (Promega, USA) with the pET-28b-hTERT plasmid. Both plasmids were kind gift from Dr Lea Harrington at the Department of Medical Biophysics, University of Toronto, Canada. Reconstitution was carried in a 50-μl volume containing 40 μl of TnT Quick Mix, 2 μl PCR enhancer, 1 μl of 1 mM methionine, 1 μg pET-28b-hTERT plasmid. After incubation at 30°C for 90 min, 2 μl 0.5 μg/μl purified hTR RNA was added to the reaction mixture, and the incubation extended for another 90 min.

Telomerase extension was carried out with 0.05 pmol G-quadruplex or control substrate (Figure 2A) in a volume of 44 μl containing 20 mM Tris–HCl (pH 8.3), 100 μM dNTP, 1.5 mM MgCl$_2$, 63 mM KCl, 1 mM EGTA, 0.005% Tween 20, 100 μg/ml bovine serum albumin (BSA) and 5 μl diluted telomerase. After 5 min

incubation at 25°C, the reaction was terminated by heating at 94°C for 5 min followed by addition of 6 μl PCR mixture containing 14 pmol of upstream primer 5′-TTGATTGGGA TTGGGATTGGGTT-3′ and 15 pmol of downstream primer 5′-GTGCCCTTACCCTTACCCTTACCCT-3′ for the extended products, 8.3 pmol of primers TS (5′-A ATCCGTCGAGCAGAGTT-3′) and NT (5′-ATCGCTT CTCGGCCTTTT-3′), 1 amol of TSNT (5′-AATCCGTC GAGCAGAGTTAAAAGGCCGAGAAGCGAT-3′) template for internal standard, and 1 U of Taq DNA polymerase (Ex Taq HotStart, TaKaRa, Dalian, China). The samples were subjected to 34 PCR cycles of 94°C for 30 s, 55°C for 30 s. Ten microliter PCR products were resolved on 12% polyacrylamide gel with an Acryl/Bis ratio of 19:1 (w/w), stained with ethidium bromide and recorded on a ChemiImager 5500 (Alpha Innotech, USA). The telomerase products for each substrate were normalized to the co-amplified internal standard and the activity ratio of G-quadruplex over control substrate was calculated to judge the effect of G-quadruplex on telomerase activity.

Dimethyl sulfate footprinting

Footprinting was carried out essentially as described (16). FAM-labeled oligonucleotide was made in 10 mM Tris–HCl (pH 7.4) buffer containing 1 mM ethylenediaminete-traacetic acid (EDTA) and 150 mM KCl or LiCl, heated at 95°C for 5 min and then cooled on ice for 10 min. Ten picomoles of FAM-labeled oligonucleotide in 100 μl volume were then mixed with 4 μl of 10% (v/v) dimethyl sulfate (DMS) in ethanol and incubated for 6 min at room temperature. The reaction was stopped by addition of 100 μl stop buffer (0.6 M NaOAc, 0.1 M β-mercapto-ethanol, 20 μg sperm DNA). After a phenol/chloroform extraction and ethanol precipitation, the oligonucleotide was dissolved in 50 μl water and mixed with 50 μl of 20% (v/v) piperidine in water. The samples were heated at 90°C for 30 min, followed by phenol/chloroform extraction and ethanol precipitation. The precipitated oligonucleotide was dissolved in 50% (v/v) deionized formamide in water, denatured at 95°C for 5 min and resolved on a denaturing 15% polyacrylamide gel.

Telomere strand invasion and extension

Telomere strand invasion and extension were analyzed as previously described (17,18) with modifications, using a pGEM-T plasmid carrying 80 T_2AG_3 repeats. Double-stranded human telomeric DNA was obtained by PCR amplification using synthetic primers 5′-(T$_2$AG$_3$)$_5$-3′ and 5′-(C$_3$TA$_2$)$_5$-3′ as described (19) and inserted into the plasmid pGEM-T Easy (Promega). The construct was transformed into *Escherichia coli* TOP10 and verified by sequencing. The plasmid (120 ng/μl) was incubated for 15 min at 25°C in extension buffer of 50 mM HEPES, pH 7.9, containing 100 μg/ml BSA, 1 mM DTT, 2% glycerol, supplied with 150 mM KCl, 15 mM MgCl$_2$, 100 μM dTTP, 100 μM dATP, 200 nM Cy5-ddGTP (GE, USA) in a volume of 9 μl. Telomeric G-rich oligonucleo-tide (Figure 3A) in extension buffer was heated at 95°C for 5 min, cooled on ice for 15 min. Then 2 μl of 500 nM (Figure 3) or 3 μM (Figure 4) oligonucleotide and 1 μl of
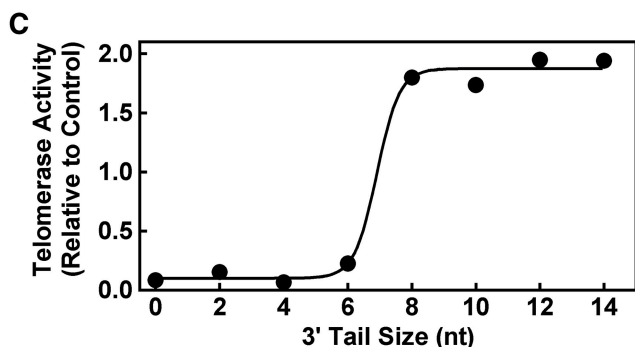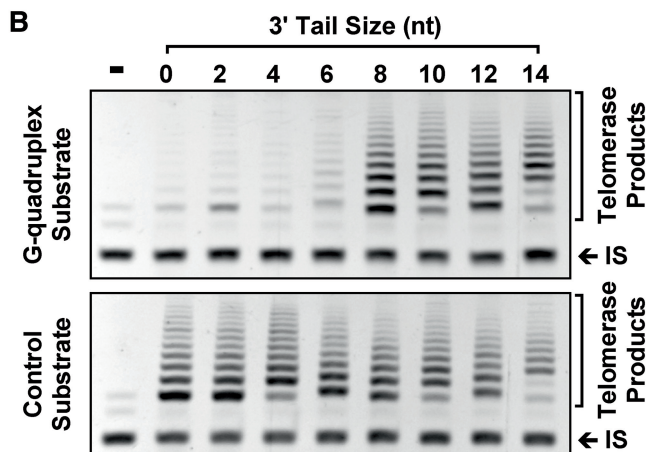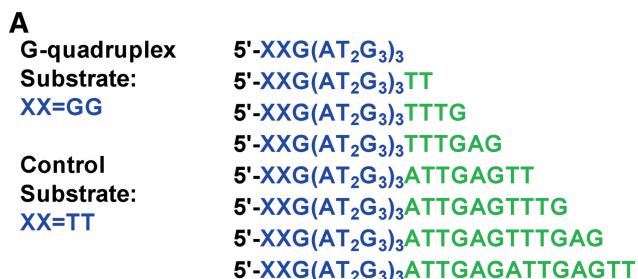
A

G-quadruplex Substrate:
XX=GG

5'-XXG(AT$_2$G$_3$)$_3$
5'-XXG(AT$_2$G$_3$)$_3$TT
5'-XXG(AT$_2$G$_3$)$_3$TTTG
5'-XXG(AT$_2$G$_3$)$_3$TTTGAG

Control Substrate:
XX=TT

5'-XXG(AT$_2$G$_3$)$_3$ATTGAGTT
5'-XXG(AT$_2$G$_3$)$_3$ATTGAGTTTG
5'-XXG(AT$_2$G$_3$)$_3$ATTGAGTTTGAG
5'-XXG(AT$_2$G$_3$)$_3$ATTGAGATTGAGTT

Figure 2. Effect of 3′ tail size on the extension of G-quadruplex substrate by telomerase assayed by the TRAP-G4 method. (**A**) G-quadruplex and control substrates used. In the control substrates, the 5′ distal GG was mutated to TT to prevent G-quadruplex formation. (**B**) Telomerase products obtained with G-quadruplex substrates (top image) and control substrates (bottom image). (**C**) Ratio of telomerase activity on G-quadruplex over control substrate as a function of 3′ tail size. Reaction buffer contained 63 mM K$^+$.

5 U Klenow fragment (exo-) (Fermentas, Lithuania) were added to the sample, respectively. After incubation at 25°C for 3.5 min, reaction was terminated by the addition of 1 µl of 10 µM (Figure 3) or 14 µM (Figure 4) 5′-(C$_3$TA$_2$)$_3$C$_3$-3′ to bind the free G-rich strand and 0.5 M EDTA to inactivate the Klenow polymerase. For analyzing oligonucleotide uptake, 4 µl of sample was mixed with 1.5 µl of 400 nM (Figure 3) or 2 µl of 1.5 µM (Figure 4) 5′-Cy3-GCAGCAGTGACCTA-GTCGACGTTTCGTC GACTAG-3′ and 2 µl of 25% Ficoll, electrophoresed on 1% agarose at 4 V/cm and Cy3 fluorescence scanned on a Typhoon 9200 scanner (GE, NJ, USA). The same gel was

then stained with ethidium bromide (EB) and recorded on a ChemiImager 5500 (Alpha Innotech, USA) for visualizing plasmid. To quantitate extension, 4 µl aliquot from the same sample was mixed with 8 µl of 3 µM 5′-T$_2$G(T$_2$AG$_3$)$_3$-3′ in deionized formamide, heated at 95°C for 5 min and electrophoresed at 20 V/cm on a 19% denaturing polyacrylamide gel containing 8 M urea. Fluorescence of incorporated Cy5-ddGTP was scanned on a Typhoon 9200 scanner. Gel analysis was carried out using the ImageQuant 5.2 software.

G-quadruplex unwinding

G-quadruplex unwinding was carried out with a truncated BLM variant, BLM[642–1296] as recently described (20) on a Spex Fluorolog-3 spectrofluorometer (HORIBA Jobin Yvon, France) at 20°C in a 2 ml volume of 150 mM or indicated K$^+$ solution with 5 nM DNA substrate.

K_F measurement of G-quadruplex on overhang

Measurements were carried out as described in 150 mM K$^+$ solution at 37°C using two ssDNA/dsDNA hybrid constructs shown in Figure 6. Details of measurement can be found in ref. 21.

RESULTS

Telomerase requires a minimal 8 nt 3′ tail beyond a G-quadruplex to extend telomere

In the telomerase-mediated telomere extension, the 3′ end of a telomere G-rich strand has to align with the RNA template in the telomerase before being extended (Figure 1) (22). The dependence of telomere extension on the size of the 3′ tail is given in Figure 2. The telomerase activity assays adopted a TRAP-G4 method (13) and used a set of G-quadruplex substrates modified to carry a single-stranded 3′ tail of various sizes with proper mutations to prevent them from participating in G-quadruplex formation and binding PCR primer (Figure 2A) (23,24). Since human telomerase can use non-telomeric DNA as substrate (25), the control substrates without G-quadruplex were all efficiently extended (Figure 2B, bottom image). In contrast, extension of G-quadruplex substrates was only obvious in those with 8 nt or longer tail (Figure 2B, top image). Using the control substrates to calibrate the effect of sequence variation at the 3′ end, the result clearly shows that human telomerase required a minimum of 8 nt tail to extend G-quadruplex substrate (Figure 2C). From this result, it is inferred that formation of G-quadruplex at the very 3′ end ensures inhibition of telomerase activity.

The G-quadruplex substrates differ not only in their tail sizes but also in their 3′ terminal sequences (Figure 2A). The influence of tail size on substrate extension is obtained by calibrating the influence of sequence variation with the control substrates that had the same terminal sequences as their corresponding G-quadruplex substrates. Another concern regarding the minimum tail requirement comes from the fact that human telomerase processes nucleolytic activity that can remove multiple residuals
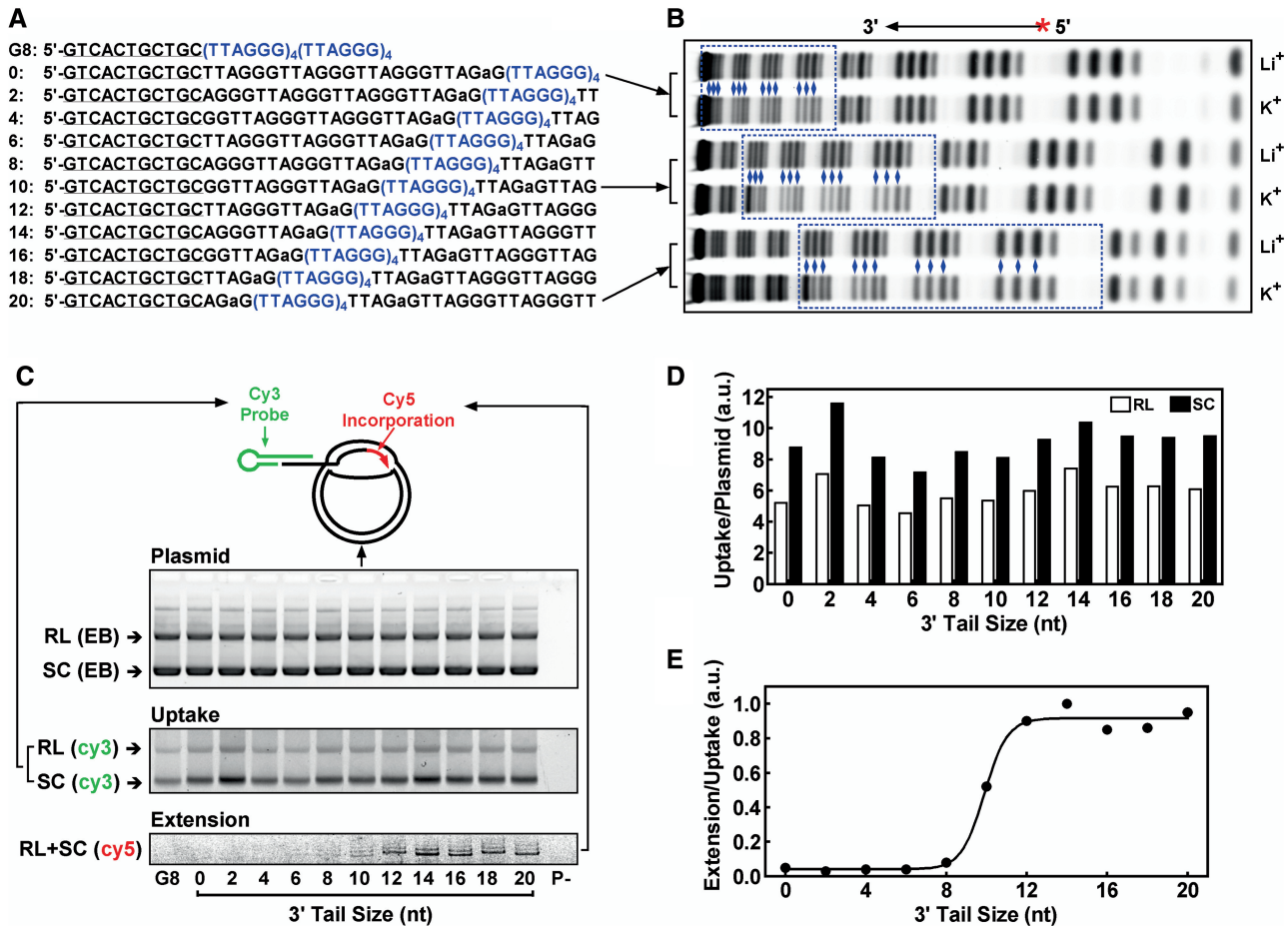
Figure 3. Effect of 3′ tail size on the invasion and extension by Klenow polymerase of G-rich telomeric oligonucleotide with G-quadruplex into telomere plasmid. (**A**) Oligonucleotides used. Lowercase 'a' indicates mutation to fix G-quadruplex formation at desired positions (blue letters). Underlined region is for stacking hybridization with a Cy3-labeled probe to visualize uptake on gel. (**B**) G-quadruplex formation in three representative oligonucleotides (0, 10, 20) revealed by reduced cleavage of guanines (blue diamonds) in the $(TTAGGG)_4$ region (blue dotted box) in DMS footprinting in K^+ versus in Li^+ solution. G-quadruplex forms in K^+ but not in Li^+ solution. (**C**) Gels from top to bottom show plasmid stained by ethidium bromide (EB), uptake of G-rich telomere DNA (labeled with Cy3-probe) and extension by Klenow polymerase (labeled by Cy5-ddGTP incorporation), respectively. The two major bands in EB staining represent the relaxed (RL) and super coiled (SC) plasmid, respectively. The lane 'P-' was the same of the 20 nt lane, but without plasmid. (**D**) Oligonucleotide uptake in relaxed (RL) and super coiled (SC) plasmid normalized by the amount of plasmid. (**E**) Quantitation of oligonucleotide extension relative to uptake as a function of 3′ tail size. Reaction buffer contained 150 mM K^+.

from the 3′ end (26). This might result in a possibility that the minimal required tail size did not represent the actual minimal tail. To clarify this possibility, the sequence of the tails in the substrates was arranged in such a way that cleavage from the 3′ end of a substrate would result in substrates matching those of shorter tails. It can be deduced that the extension of the 8-nt tail substrate was not generated from its nucleolytic products because the substrates with shorter tails were not extended. Similar tail size requirement has been reported of duplex DNA substrate for which human telomerase required 6–9 nt overhang for extension (27).

Invaded telomere strand requires a minimal 12 nt 3′ tail beyond a G-quadruplex for extension

In certain telomerase-negative cells, telomere extension is fulfilled by the ALT pathway in which the 3′ end of a telomere strand invades the duplex region of telomeric DNA and hybridizes to the C-rich strand for extension (Figure 7B, right) (28). The strand invasion of telomere DNA has been studied *in vitro* by analyzing the uptake of single-stranded G-rich oligonucleotide into plasmid containing telomere sequence (17,18). By incubating G-rich telomere strands with a plasmid containing 80 T_2AG_3 repeats, we studied how the 3′ tail size could affect their uptake and subsequent extension by the Klenow polymerase. The G-rich strands were of identical length carrying a G-quadruplex at different positions to produce a 3′ single-stranded tail of 0–20 nt (Figure 3A). G-quadruplex formation was constrained to four consecutive TTAGGG repeats at intended positions by a G to A mutation in the two neighboring repeats and confirmed by DMS footprinting in which the guanines participated in G-quadruplex formation was protected from methylation resulting in less cleavage relative to those in the control (Figure 3B). A more intense band for the guanine at the
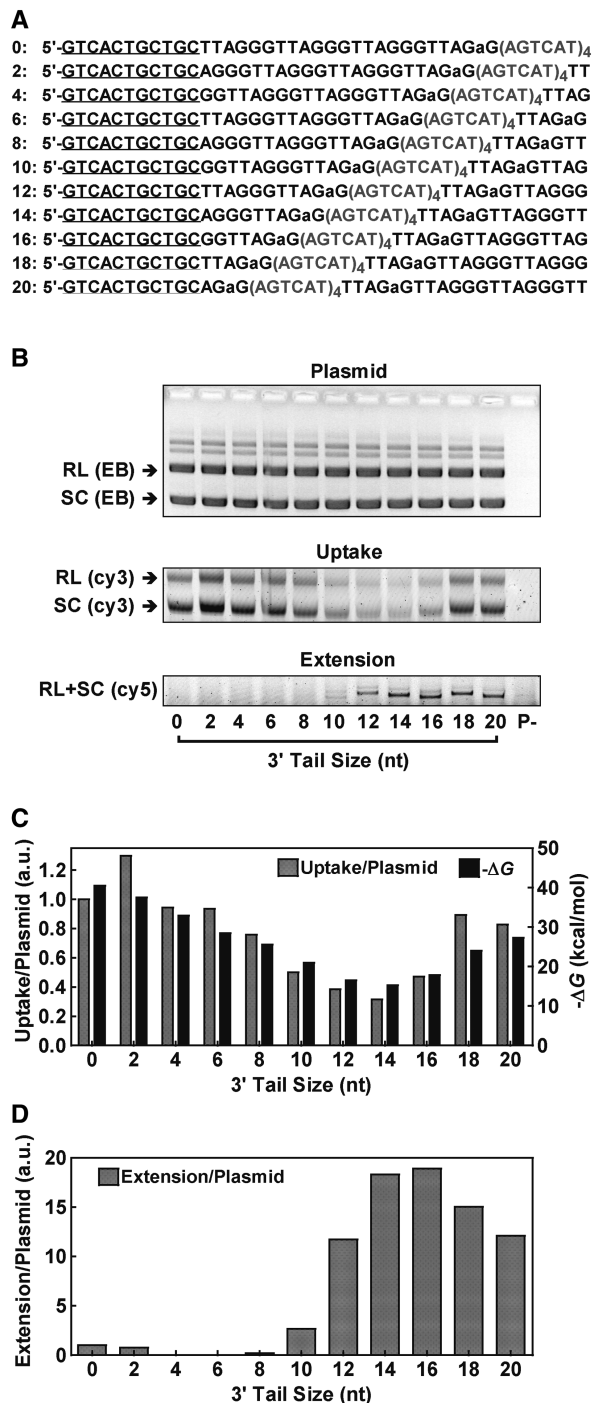
A

```
0:  5'-GTCACTGCTGCTTAGGGTTAGGGTTAGGGTTAGaG(AGTCAT)4
2:  5'-GTCACTGCTGCAGGGTTAGGGTTAGGGTTAGaG(AGTCAT)4TT
4:  5'-GTCACTGCTGCGGTTAGGGTTAGGGTTAGaG(AGTCAT)4TTAG
6:  5'-GTCACTGCTGCTTAGGGTTAGGGTTAGaG(AGTCAT)4TTAGaG
8:  5'-GTCACTGCTGCAGGGTTAGGGTTAGaG(AGTCAT)4TTAGaGTT
10: 5'-GTCACTGCTGCGGTTAGGGTTAGaG(AGTCAT)4TTAGaGTTAG
12: 5'-GTCACTGCTGCTTAGGGTTAGaG(AGTCAT)4TTAGaGTTAGGG
14: 5'-GTCACTGCTGCAGGGTTAGaG(AGTCAT)4TTAGaGTTAGGGTT
16: 5'-GTCACTGCTGCGGTTAGaG(AGTCAT)4TTAGaGTTAGGGTTAG
18: 5'-GTCACTGCTGCTTAGaG(AGTCAT)4TTAGaGTTAGGGTTAGGG
20: 5'-GTCACTGCTGCAGaG(AGTCAT)4TTAGaGTTAGGGTTAGGGTT
```

B

C

D

Figure 4. Effect of 3′ tail size on the invasion and extension by Klenow polymerase of G-rich telomeric oligonucleotide without G-quadruplex into telomere plasmid. (**A**) Oligonucleotides used, which are the same as those in Figure 3 except that the $(TTAGGG)_4$ region was mutated into $(AGTCAT)_4$ to abolish formation of G-quadruplex. (**B**) Gels from top to bottom show plasmid stained by ethidium bromide (EB), uptake of G-rich telomere DNA (labeled with Cy3-probe) and extension by Klenow polymerase (labeled by Cy5-ddGTP incorporation), respectively. The two major bands in EB staining represent the relaxed (RL) and super coiled (SC) plasmid, respectively. The lane 'P-' was the same of the 20 nt band, but without plasmid. (**C**) Uptake of oligonucleotide normalized by the amount of plasmid and ΔG of oligonucleotide hybridization with plasmid (calculated using the online Hetero Dimer tool of OligoAnalyzer at http://www.idtdna.com/). (**D**) Oligonucleotide extension normalized by the amount of plasmid. Reaction buffer contained 150 mM K^+.

3′ end of G-quadruplex was noticed. This might be caused by effects similar to those that produce hypercleavage to the guanine at the interface of structural transition of DNA in DMS footprinting (29). Although formation of G-quadruplex with TTAGaGTTA or longer loops could not be excluded, our previous study showed that such quadruplexes have very low stability and should be in much smaller amount comparing to the G-quadruplex with only TTA loops (10).

The uptake was probed with a Cy3-labeled hairpin oligonucleotide via stacking hybridization (30) and the templated extension was labeled by incorporation of Cy5-ddGTP (Figure 3C). They were then resolved on agarose and denaturing polyacrylamide gel, respectively, and quantitated by the fluorescence of the two dyes calibrated to the amount of oligonucleotide uptaken. While the tail size had a minor influence on the uptake (Figure 3D), the extension clearly showed a requirement of a minimal tail of 12 nt (Figure 3E). The ddGTP was used to ensure that each extended oligonucleotide was labeled by a single Cy5 dye. The major extension band was followed by a weak one on the gel (Figure 3C, bottom image). This could be caused by possible dGTP contamination from the other two dNTPs. It is noted that the uptake by the supercoiled plasmid was significantly greater than that by the relaxed plasmid (Figure 3D). This result suggests that the annealing of oligonucleotide was facilitated in the former structure and is consistent with the observation that the telomere dsDNA-binding protein, TRF2, which increases the superhelical density of telomere plasmid, enhanced strand invasion (17).

To further examine how the presence of G-quadruplex affect the extension by Klenow polymerase, uptake and extension were also assayed using oligonucleotides with the $(TTAGGG)_4$ region mutated so they did not form G-quadruplex (Figure 4A). In contrast to those in the previous experiment, these oligonucleotides associated with the plasmid in the gel displayed large variation (Figure 4B), which correlates with the calculated ΔG, the change of free energy reflecting the stability of hybridization between the oligonucleotides and plasmid (Figure 4C). The decreased association of oligonucleotides with tails around 14 nt can be explained by their dissociation during later sample processing such as electrophoresis, because the 24-nt mutation segment was unable to anneal with the plasmid. While the uptake and extension were permitted in a few minutes, the sample processing followed took much longer time. After the uptake and extension reaction was stopped, the presence of excessive amount of C-rich oligonucleotide prevented further uptake of G-rich oligonucleotides and trapped those dissociated from plasmid. The dissociation was more difficult to occur for the G-quadruplex-forming oligonucleotides. After the reactions were stopped, the G-quadruplex in them might unfold and anneal with the plasmid because it cannot compete with duplex formation in dilute solution (16); therefore, these oligonucleotides could remain associated with the plasmid during sample processing. For these reasons, it is rational to assume that the mutated oligonucleotides were uptaken in similar amount and the extension normalized on plasmid amount given in Figure 4D

should largely reflect the actual extension efficiency of these oligonucleotides. The requirement of about a 12-nt tail for extension seen in both Figures 3E and 4D in the presence and absence of G-quadruplex implies that the Klenow polymerase itself required a minimal size of priming for extension and G-quadruplex formation at the 3′ end can limit extension by affecting the size of priming.

BLM helicase requires a minimal 3′ tail of 6 nt beyond a G-quadruplex for unwinding

DNA helicases are motor proteins involved in resolving DNA secondary structure, which is required in processes such as DNA replication and transcription. We examined the influence of the 3′ tail size on the unwinding of G-quadruplex by the BLM helicases using a real-time method we recently reported (20). BLM is a member of the RecQ family of DNA helicases that unwind DNA in a 3′→5′ direction by consumption of ATP as an energy source (31). It requires a single-stranded region for loading itself onto substrate before executing unwinding (32) and G-quadruplex DNA is a preferred substrate (33). Unwinding assays were first performed with a duplex substrate carrying 3′ $(T_2AG_3)_4$ tail (Figure 5A) by monitoring the increase in fluorescence upon the separation of the duplex (Figure 5B) (20). In the absence of K^+, the tail did not form G-quadruplex such that the helicase could load onto it to unwind the duplex. G-quadruplex is expected to prevent the loading of helicase and, as a result, the unwinding of duplex as well (Figure 5B). Indeed, when G-quadruplex formation was promoted by increasing concentration of K^+, the unwinding became increasingly inhibited (Figure 5C). This result showed that G-quadruplex without a tail is not substrate for the BLM helicase.

We then added additional tail of various sizes to the 3′ side of the G-quadruplex forming region and carried out unwinding assays in 150 mM K^+ solution. The added tails were of random sequence so that the substrate here was a
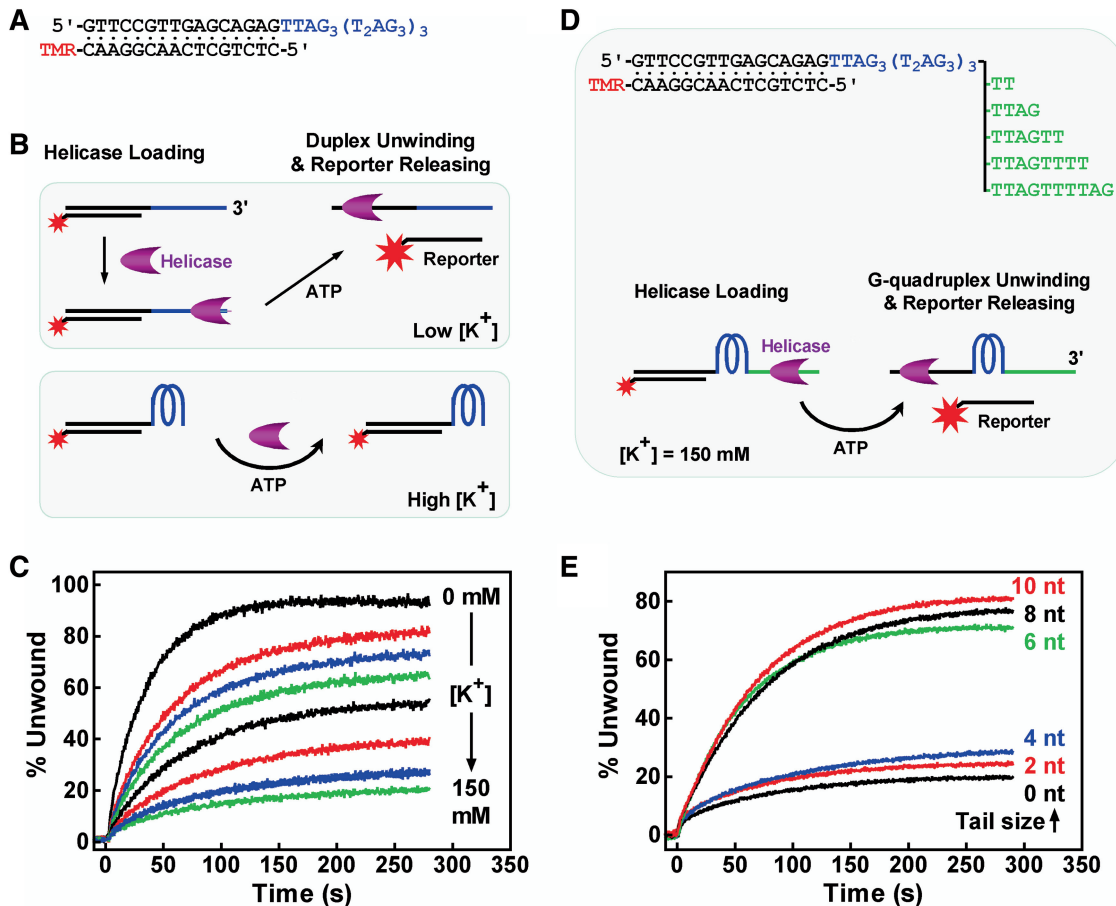

Figure 5. Effect of 3′ tail size on the unwinding of G-quadruplex by BLM helicase. (**A**) Duplex substrate flanked by a 3′ $(T_2AG_3)_4$ tail capable of forming G-quadruplex in the presence of K^+. (**B**) Scheme showing expected effect of G-quadruplex formation on the unwinding of duplex. Unwinding of duplex releases the probe labeled with a fluorescent dye tetramethylrhodamine (TMR). The dye is quenched in duplex by the guanine at the opposite strand and becomes fluorescent upon duplex unwinding. (**C**) Unwinding kinetics of duplex at various concentrations of K^+. Li^+ was supplied to make the final concentration of mono cations to 150 mM. (**D**) G-quadruplex substrates with single-stranded 3′ tails of 0, 2, 4, 6, 8 and 10 nt and unwinding scheme. Unwinding of G-quadruplex followed by a duplex leads to increase in TMR fluorescence as a result of reporter releasing. (**E**) Unwinding kinetics of G-quadruplex carrying a 3′ tail of indicated size. Percent of unwinding was calculated as $100 \times \Delta F/\Delta F_{max}$, where ΔF is the increase in fluorescence at a given time and ΔF_{max} the difference of fluorescence between the reporter in the bound and fully released form (20).

$G_3(T_2AG_3)_3$ G-quadruplex with a duplex at the 5′ side carrying a fluorescent reporter and a single-stranded tail of various sizes at the 3′ side (Figure 5D). Successive unwinding of the G-quadruplex and duplex was reflected by the increase in fluorescence when the fluorescent reporter was released. The results showed that the unwinding remained low for substrates with of 0–4 nt tails, but dramatically jumped to high efficiency when the tails increased to 6 nt or longer (Figure 5E). This result indicates that the helicase required a minimum of 6 nt tail for efficient unwinding of the telomere G-quadruplex. Taken together, our results on the unwinding assays show that G-quadruplex at the very 3′ end will be resistant to the unwinding activity of the BLM helicase and likely other resolving activities working with similar mechanisms.

Folding equilibrium constant of G-quadruplex at the 3′ of telomere overhang

We have previously reported that telomere G-quadruplex tends to form at the very 3′ end of telomere overhang (10). The above-mentioned results show that such G-quadruplex formation inhibits the extension of telomere by either telomerase or the ALT mechanism, as well as its unwinding. To obtain more quantitative information on the possibility of adopting a folded or relaxed state by telomere DNA when it is liberated, we further measured the folding equilibrium constant K_F of telomere G-quadruplex at the 3′ end of telomere overhang in an ssDNA/dsDNA construct that mimics the chromosome end structure (Figure 6A) using an isothermal differential hybridization (IDH) method (21). The IDH method uses a probe oligonucleotide to hybridize the major part of the G-quadruplex-forming region of an analyte oligonucleotide and the same region of a reference oligonucleotide that is unable to form G-quadruplex because of the mutation outside of the hybridization region. The formation of G-quadruplex in the analyte oligonucleotide leads to a reduced hybridization relative to that of the reference oligonucleotide. The K_F of the G-quadruplex can then be obtained from the difference in hybridization between the analyte and reference oligonucleotide.

The scheme given in Figure 6A shows the two sets of hybridizations with the analyte and reference oligonucleotides, respectively. The two hybridization curves are given in Figure 6B, which yielded a K_F of 110.9 for the analyte oligonucleotide. Compared with the free $G_3(T_2AG_3)_3$ that showed a K_F of 807.5 in our previous work (21), this much smaller K_F indicates that the G-quadruplex in the overhang was significantly destabilized due to the presence of flanking structures. This property is in agreement with the observation that adjacent association with protein destabilizes G-quadruplex (21). A human cell processes 92 telomere ends. A K_F of 110.9 for the G-quadruplex on overhang would mean that less than one telomere 3′ end in a cell would by itself assume an unfolded form when liberated free. The intracellular environment is crowded with mass of biomolecules. Molecular crowding can dramatically enhance the thermal stability of telomere G-quadruplex (16,34,35) by as much as 20°C (16). Therefore the K_F for the G-quadruplex at the 3′
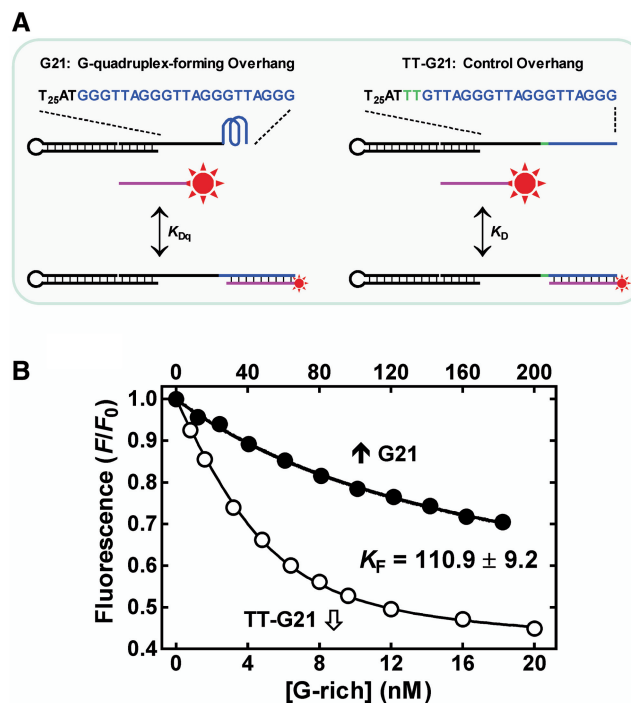

Figure 6. Measurement of K_F for G-quadruplex formed by $G_3(T_2AG_3)_3$ on the 3′ end of single-stranded G-rich overhang in a ssDNA/dsDNA hybrid construct by the IDH method (21). (**A**) Scheme of reactions. A 5-carboxyfluorescein (FAM, star) labeled C-rich DNA probe (purple) was hybridized to the $G(T_2AG_3)_2T_2AG_2$ region in the G-quadruplex-forming (G21) and the non-G-quadruplex forming (TT-G21) overhangs, respectively, in 150 mM K^+ solution. Hybridization quenched the fluorescence of the FAM at the 5′ end of the C-rich DNA. (**B**) Representative hybridization curves from which the dissociation constant K_{Dq} and K_D was derived, respectively. The K_F was obtained as $K_{Dq}/K_D - 1$ (21) and expressed as the mean of three measurements.

telomere end *in vivo* may be even greater to disfavor the unfolded form.

DISCUSSION

With a repeating unit of T_2AG_3 and four such repeats being able to form G-quadruplex, human telomere overhang can, in principle, end with a single-stranded 3′ tail ranging from 0 to 23 nt. Our data show that the telomerase and Klenow polymerase require a minimal 8 and 12 nt tail for extending telomere DNA, respectively, and the BLM helicase requires a minimal 6 nt tail for unwinding G-quadruplex. The preferential formation of G-quadruplex at the farthest 3′ end (10) minimizes the tail to no more than 5 nt that is shorter than the required minimal tail size of the above reactions we studied (Figures 2–5). If G-quadruplex would form randomly along the G-rich overhang, then the majority of telomere ends would not be inhibitory. The preferential formation of G-quadruplex at the 3′ telomere end and a sufficiently large K_F (Figure 6) apparently provide a molecular basis for the inhibition of these end-processing reactions.
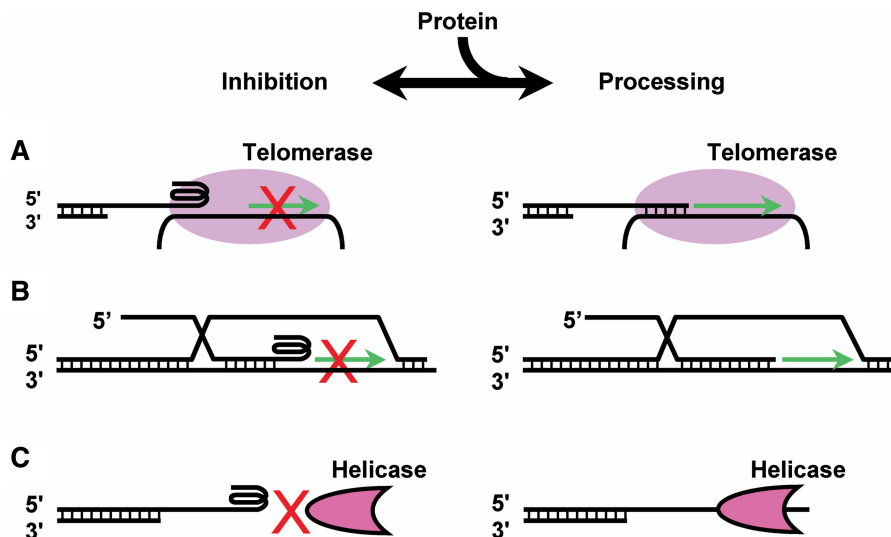
Figure 7. Biological implications of telomere ending structure. Preferential formation of G-quadruplex at the very 3′ end of G-rich overhang is inhibitory to telomere processing that requires a free single-stranded 3′ tail, such as telomere extension by (**A**) telomerase or (**B**) the alternative lengthening of telomeres (ALT) and (**C**) unwinding by activities like helicases (schemes at left). G-quadruplex disruption by proteins may remove the inhibition to permit telomere end processing (schemes at right). The counteracting of G-quadruplex formation and unfolding by proteins may regulate the accessibility of the 3′ telomere end in various processes.

The 3′ preference of G-quadruplex formation may have implications in two aspects (Figure 7). First, it may provide G-quadruplex the ability to play regulatory roles in those reactions where a free telomere 3′ end is required. The presence of telomere G-quadruplex *in vivo* has been supported by several evidences (36–38). G-rich sequences in genomic DNA have been shown to form G-quadruplex structures during RNA transcription even when they are constrained in DNA duplex (16). Human telomere G-quadruplex can be unfolded by several proteins (39,40) or destabilized by adjacent protein (21). The co-ordination between G-quadruplex formation at the 3′ end and their unfolding by proteins may determine the availability of the telomere 3′ end in events such as telomere extension and unwinding. Second, the preferential formation at the very 3′ end makes G-quadruplex a unique target for the disruption of telomere length maintenance in cancer cells. While the majority of tumor cells rely on telomerase for telomere maintenance, a small fraction uses the ALT mechanism. Thus, targeting telomerase may risk inducing or selecting for activation of the ALT mechanism (28). Since G-quadruplex at the 3′ telomere end is inhibitory to both telomerase and the ALT mechanism, the above concern may be avoided when G-quadruplex is targeted.

REFERENCES

1. Makarov,V.L., Hirose,Y. and Langmore,J.P. (1997) Long G tails at both ends of human chromosomes suggest a C strand degradation mechanism for telomere shortening. *Cell*, **88**, 657–666.
2. Wright,W.E., Tesmer,V.M., Huffman,K.E., Levene,S.D. and Shay,J.W. (1997) Normal human chromosomes have long G-rich telomeric overhangs at one end. *Genes Dev.*, **11**, 2801–2809.
3. Zhao,Y., Hoshiyama,H., Shay,J.W. and Wright,W.E. (2008) Quantitative telomeric overhang determination using a double-strand specific nuclease. *Nucleic Acids Res.*, 36, e14.
4. Chai,W., Du,Q., Shay,J.W. and Wright,W.E. (2006) Human telomeres have different overhang sizes at leading versus lagging strands. *Mol. Cell*, **21**, 427–435.
5. Olovnikov,A.M. (1973) A theory of marginotomy. The incomplete copying of template margin in enzymic synthesis of polynucleotides and biological significance of the phenomenon. *J. Theor. Biol.*, **41**, 181–190.
6. Morin,G.B. (1997) Telomere control of replicative lifespan. *Exp. Gerontol.*, **32**, 375–382.
7. Kim,N.W., Piatyszek,M.A., Prowse,K.R., Harley,C.B., West,M.D., Ho,P.L., Coviello,G.M., Wright,W.E., Weinrich,S.L. and Shay,J.W. (1994) Specific association of human telomerase activity with immortal cells and cancer. *Science*, **266**, 2011–2015.
8. Zahler,A.M., Williamson,J.R., Cech,T.R. and Prescott,D.M. (1991) Inhibition of telomerase by G-quartet DNA structures. *Nature*, **350**, 718–720.

9. Neidle,S. (2010) Human telomeric G-quadruplex: the current status of telomeric G-quadruplexes as therapeutic targets in human cancer. *FEBS J.*, **277**, 1118–1125.

10. Tang,J., Kan,Z.Y., Yao,Y., Wang,Q., Hao,Y.H. and Tan,Z. (2008) G-quadruplex preferentially forms at the very 3' end of vertebrate telomeric DNA. *Nucleic Acids Res.*, **36**, 1200–1208.

11. Beattie,T.L., Zhou,W., Robinson,M.O. and Harrington,L. (1998) Reconstitution of human telomerase activity *in vitro*. *Curr. Biol.*, **8**, 177–180.

12. Weinrich,S.L., Pruzan,R., Ma,L., Ouellette,M., Tesmer,V.M., Holt,S.E., Bodnar,A.G., Lichtsteiner,S., Kim,N.W., Trager,J.B. *et al*. (1997) Reconstitution of human telomerase with the template RNA component hTR and the catalytic protein subunit hTRT. *Nat. Genet.*, **17**, 498–502.

13. Gomez,D., Mergny,J.L. and Riou,J.F. (2002) Detection of telomerase inhibitors based on g-quadruplex ligands by a modified telomeric repeat amplification protocol assay. *Cancer Res.*, **62**, 3365–3368.

14. Kim,N.W. and Wu,F. (1997) Advances in quantification and characterization of telomerase activity by the telomeric repeat amplification protocol (TRAP). *Nucleic Acids Res.*, **25**, 2595–2597.

15. Yao,Y., Wang,Q., Hao,Y.H. and Tan,Z. (2007) An exonuclease I hydrolysis assay for evaluating G-quadruplex stabilization by small molecules. *Nucleic Acids Res.*, **35**, e68.

16. Zheng,K.W., Chen,Z., Hao,Y.H. and Tan,Z. (2010) Molecular crowding creates an essential environment for the formation of stable G-quadruplexes in long double-stranded DNA. *Nucleic Acids Res.*, **38**, 327–338.

17. Amiard,S., Doudeau,M., Pinte,S., Poulet,A., Lenain,C., Faivre-Moskalenko,C., Angelov,D., Hug,N., Vindigni,A., Bouvet,P. *et al.* (2007) A topological mechanism for TRF2-enhanced strand invasion. *Nat. Struct. Mol. Biol.*, **14**, 147–154.

18. Pedroso,I.M., Hayward,W. and Fletcher,T.M. (2009) The effect of the TRF2 N-terminal and TRFH regions on telomeric G-quadruplex structures. *Nucleic Acids Res.*, **37**, 1541–1554.

19. Ijdo,J.W., Wells,R.A., Baldini,A. and Reeders,S.T. (1991) Improved telomere detection using a telomere repeat probe (TTAGGG)n generated by PCR. *Nucleic Acids Res.*, **19**, 4780.

20. Liu,J.Q., Chen,C.Y., Xue,Y., Hao,Y.H. and Tan,Z. (2010) G-quadruplex hinders translocation of BLM helicase on DNA: a real-time fluorescence spectroscopic unwinding study and comparison with duplex substrates. *J. Am. Chem. Soc.*, **132**, 10521–10527.

21. Wang,Q., Ma,L., Hao,Y.H. and Tan,Z. (2010) Folding equilibrium constants of telomere g-quadruplexes in free state or associated with proteins determined by isothermal differential hybridization. *Anal. Chem.*, **82**, 9469–9475.

22. Gavory,G., Farrow,M. and Balasubramanian,S. (2002) Minimum length requirement of the alignment domain of human telomerase RNA to sustain catalytic activity *in vitro*. *Nucleic Acids Res.*, **30**, 4470–4480.

23. Yanez,G.H., Khan,S.J., Locovei,A.M., Pedroso,I.M. and Fletcher,T.M. (2005) DNA structure-dependent recruitment of telomeric proteins to single-stranded/double-stranded DNA junctions. *Biochem. Biophys. Res. Commun.*, **328**, 49–56.

24. Qi,H., Lin,C.P., Fu,X., Wood,L.M., Liu,A.A., Tsai,Y.C., Chen,Y., Barbieri,C.M., Pilch,D.S. and Liu,L.F. (2006) G-quadruplexes induce apoptosis in tumor cells. *Cancer Res.*, **66**, 11808–11816.

25. Morin,G.B. (1991) Recognition of a chromosome truncation site associated with alpha-thalassaemia by human telomerase. *Nature*, **353**, 454–456.

26. Huard,S. and Autexier,C. (2004) Human telomerase catalyzes nucleolytic primer cleavage. *Nucleic Acids Res.*, **32**, 2171–2180.

27. Rivera,M.A. and Blackburn,E.H. (2004) Processive utilization of the human telomerase template: lack of a requirement for template switching. *J. Biol. Chem.*, **279**, 53770–53781.

28. Henson,J.D., Neumann,A.A., Yeager,T.R. and Reddel,R.R. (2002) Alternative lengthening of telomeres in mammalian cells. *Oncogene*, **21**, 598–610.

29. Drouin,R., Therrien,J.P., Angers,M. and Ouellet,S. (2001) *In vivo* DNA analysis. *Methods Mol. Biol.*, **148**, 175–219.

30. Yuan,B.F., Zhuang,X.Y., Hao,Y.H. and Tan,Z. (2008) Kinetics of base stacking-aided DNA hybridization. *Chem. Commun.*, 6600–6602.

31. Karow,J.K., Chakraverty,R.K. and Hickson,I.D. (1997) The Bloom's syndrome gene product is a 3′-5′ DNA helicase. *J. Biol. Chem.*, **272**, 30611–30614.

32. Sun,H., Karow,J.K., Hickson,I.D. and Maizels,N. (1998) The Bloom's syndrome helicase unwinds G4 DNA. *J. Biol. Chem.*, **273**, 27587–27592.

33. Hickson,I.D. (2003) RecQ helicases: caretakers of the genome. *Nat. Rev. Cancer*, **3**, 169–178.

34. Xue,Y., Kan,Z.Y., Wang,Q., Yao,Y., Liu,J., Hao,Y.H. and Tan,Z. (2007) Human telomeric DNA forms parallel-stranded intramolecular G-quadruplex in K+ solution under molecular crowding condition. *J. Am. Chem. Soc.*, **129**, 11185–11191.

35. Kan,Z.Y., Lin,Y., Wang,F., Zhuang,X.Y., Zhao,Y., Pang,D.W., Hao,Y.H. and Tan,Z. (2007) G-quadruplex formation in human telomeric (TTAGGG) (4) sequence with complementary strand in close vicinity under molecularly crowded condition. *Nucleic Acids Res.*, **35**, 3646–3653.

36. Schaffitzel,C., Berger,I., Postberg,J., Hanes,J., Lipps,H.J. and Pluckthun,A. (2001) *In vitro* generated antibodies specific for telomeric guanine-quadruplex DNA react with *Stylonychia lemnae* macronuclei. *Proc. Natl Acad. Sci. USA*, **98**, 8572–8577.

37. Paeschke,K., Simonsson,T., Postberg,J., Rhodes,D. and Lipps,H.J. (2005) Telomere end-binding proteins control the formation of G-quadruplex DNA structures in vivo. *Nat. Struct. Mol. Biol.*, **12**, 847–854.

38. Zhang,M.L., Tong,X.J., Fu,X.H., Zhou,B.O., Wang,J., Liao,X.H., Li,Q.J., Shen,N., Ding,J. and Zhou,J.Q. (2010) Yeast telomerase subunit Est1p has guanine quadruplex-promoting activity that is required for telomere elongation. *Nat. Struct. Mol. Biol.*, **17**, 202–209.

39. Enokizono,Y., Konishi,Y., Nagata,K., Ouhashi,K., Uesugi,S., Ishikawa,F. and Katahira,M. (2005) Structure of hnRNP D complexed with single-stranded telomere DNA and unfolding of the quadruplex by heterogeneous nuclear ribonucleoprotein D. *J. Biol. Chem.*, **280**, 18862–18870.

40. Lipps,H.J. and Rhodes,D. (2009) G-quadruplex structures: in vivo evidence and function. *Trends Cell Biol.*, **19**, 414–422.